Published in final edited form as:
Cell. 2012 May 25; 149(5): 1125–1139. doi:10.1016/j.cell.2012.03.039.

A distal axonal cytoskeleton forms an intra-axonal boundary that controls axon initial segment assembly

Mauricio R. Galiano[1,†], **Smita Jha**[1,†], **Tammy SzuYu Ho**[2], **Chuansheng Zhang**[1], **Yasuhiro Ogawa**[1,§], **Kae-Jiun Chang**[2], **Michael C. Stankewich**[3], **Peter J. Mohler**[4], and **Matthew N. Rasband**[1,2,*]

[1]Department of Neuroscience, Baylor College of Medicine, Houston, TX 77030

[2]Program in Developmental Biology, Baylor College of Medicine, Houston, TX 77030

[3]Department of Pathology, Yale University, New Haven, CT 06520

[4]Dorothy M. Davis Heart and Lung Research Institute, Ohio State University Medical Center, Columbus, OH 43210

SUMMARY

AnkyrinG (ankG) is highly enriched in neurons at axon initial segments (AIS) where it clusters Na + and K+ channels and maintains neuronal polarity. How ankG becomes concentrated at the AIS is unknown. Here, we show that as neurons break symmetry, they assemble a distal axonal submembranous cytoskeleton comprised of ankyrinB (ankB), αII spectrin, and βII spectrin that defines a boundary limiting ankG to the proximal axon. Experimentally moving this boundary altered the length of ankG staining in the proximal axon, whereas disruption of the boundary through silencing of ankB, αII spectrin, or βII spectrin expression blocked AIS assembly and permitted ankG to redistribute throughout the distal axon. In support of an essential role for the distal cytoskeleton in ankG clustering, we also found that αII and βII spectrin -deficient mice had disrupted AIS. Thus, the distal axonal cytoskeleton functions as an intra-axonal boundary restricting ankG to the AIS.

INTRODUCTION

The final integration of synaptic inputs and initiation of action potential (AP) output occurs at the axon initial segment (AIS) due to high densities of voltage-gated Na+ and K+ channels (Kole and Stuart, 2012). AIS ion channels are clustered through interactions with the scaffolding protein ankyrinG (ankG) (Garrido et al., 2003; Pan et al., 2006). AnkG links AIS membrane proteins to the βIV spectrin and actin-based submembranous cytoskeleton (Bennett and Baines, 2001; Yang et al., 2007). Consistent with its role as the ‘master-

*Correspondence should be addressed to: Dr. Matthew N. Rasband, PhD, Department of Neuroscience, Baylor College of Medicine, One Baylor Plaza, Houston, TX 77030, Rasband@bcm.edu, phone: 713-798-4494, FAX: 713-798-3946.
†These authors contributed equally to this work.
§Present address: Department of Pharmacology, Meiji Pharmaceutical University, Tokyo, Japan, 204-8588.

Supplemental Information
Supplemental Information includes two figures and Supplemental Experimental Procedures and can be found with this article online.

organizer' of the AIS, loss of ankG disrupts AIS molecular assembly and neuronal function (Zhou et al., 1998).

AnkG's strategic location at the AIS is necessary for neurons to maintain axonal and dendritic polarity (Rasband, 2010). For example, loss of ankG from polarized neurons causes axons to acquire multiple dendritic features including dendritic cargoes, dendritic membrane and cytoplasmic proteins, and even the elaboration of spines (Hedstrom et al., 2008; Sobotzik et al., 2009; Song et al., 2009). Nervous system injuries such as stroke lead to calpain-dependent proteolysis of ankG, and the subsequent loss of neuronal polarity and ion channel clustering (Schafer et al., 2009).

The AIS functions as a site of neuronal plasticity, since disease, chronic depolarization or synaptic deprivation causes changes in AIS Na+ channel localization, leading to altered excitability (Grubb and Burrone, 2010; Kaphzan et al., 2011; Kuba et al., 2010). However, the mechanisms regulating AIS plasticity remain unknown. Phylogenetic analysis of AIS ion channels suggests that the origin of ankG-dependent ion channel clustering in early chordates was a key event that permitted the evolution of myelin, saltatory conduction, and the complex vertebrate nervous system (Hill et al., 2008).

Although these data emphasize the exceptional importance of ankG clustering at the AIS, the mechanisms responsible have remained unknown. Since ankG is also enriched at nodes of Ranvier, understanding how ankG is clustered in myelinated axons might provide clues about its AIS accumulation. During myelination, glial cells direct clustering of the cell adhesion molecule neurofascin-186 (NF-186) along axons. NF-186 then functions as a membrane receptor to cluster ankG. Finally, ankG recruits nodal ion channels (Dzhashiashvili et al., 2007; Feinberg et al., 2010; Sherman et al., 2005). In contrast, ankG clustering at the AIS during development is an intrinsic property of neurons requiring neither glial cells nor NF-186 (Hedstrom et al., 2007; Zonta et al., 2011) and must therefore depend on mechanisms distinct from those at nodes of Ranvier.

Here, we show axon specification during development precedes ankG clustering. This prompted us to search for early events in axonogenesis that contribute to ankG clustering. We identified a distal, ankG-independent submembranous axonal cytoskeleton whose assembly precedes ankG clustering, and functions as an intra-axonal boundary to restrict ankG to the proximal region of the axon. Thus, ankG clustering at the AIS occurs through an unanticipated exclusion mechanism rather than through active recruitment.

RESULTS

Axon specification precedes AIS clustering of ankG

AnkG is essential for assembly of the AIS, and for the polar distribution of many axonal and somatodendritic proteins (Rasband, 2010). However, the relationship between ankG clustering and axon specification *in vivo* has not been described. Therefore, we performed *in utero* electroporation of GFP in embryonic day 14 (E14) mouse embryos to label neurons and trace their subsequent development as they migrated through the cortical plate and arrived in layers II–III of the cortex. We collected brains at various time points after electroporation, and immunostained sections for ankG. At E16, GFP-labeled neurons had not yet entered the cortical plate, were multipolar, and lacked ankG immunostaining (Figures 1A, 1B, and 1K). By E18 many neurons could be found migrating through the cortical plate (Figures 1C and 1K). These neurons had leading and trailing processes (Figure 1D, arrowheads), with the latter becoming axons (Barnes and Polleux, 2009). Importantly, these neurons also lacked axonal ankG immunoreactivity (Figures 1D, arrowheads, and 1K). By postnatal day 1 (P1), most neurons had arrived at their final destinations in the cortex

(Figures 1E and 1K), and began to show ankG immunoreactivity at the proximal axon (Figures 1F, arrowheads and 1K). Furthermore, as neurons arrived in layers II–III of the cortex, they developed basal dendrites (Figure 1L). By P5 and P28 all GFP-labeled neurons had an AIS defined by high densities of ankG (Figures 1G, 1H, 1I, 1J, and 1K). Thus, ankG clustering occurs after axon specification.

When we measured the length and position of ankG along the axon, at both P1 and P5 we noted that the distal end of ankG staining always occurred a fixed distance from the cell body (Figure 1M), suggesting the existence of a boundary or border that determined the location of the distal end of the AIS. At P1, we found that ankG clustering appeared ~10 μm from the cell body resulting in a shorter AIS (Figures 1F, bracket, 1M, and 1N), whereas at P5 ankG staining began immediately adjacent to the neuronal cell body (Figures 1H, 1M, and 1N). Thus, the AIS matures by ankG clustering along the axon in a distal to proximal direction.

AnkG is not required for axon specification

To determine if ankG is required to establish neuronal polarity and/or axon specification independently of its accumulation and clustering at the AIS, we electroporated *in utero* a highly efficient ankG-specific shRNA (Hedstrom et al., 2007) into rat embryos, then determined whether these neurons developed axons that projected to the contralateral cortex through the c*orpus callosum*. At both P4 and P28, electroporated neurons had no detectable ankG (Figures S1A and S1B). However, these neurons still had axons that crossed the c*orpus callosum* (Figure 1O). Consistent with ankG's previously reported role in maintaining neuronal polarity (Hedstrom et al., 2008), P28 neurons lacking ankG also had spine-like protrusions along the axon (Figures S1B and S1C, arrowheads). These results show that in contrast to mature neurons, during development ankG is required neither for initiation of polarity nor axon specification.

Axons have a distinct distal membrane skeleton

The observation that ankG staining began a fixed distance from the cell body prompted us to search for proteins that might demarcate a boundary, or barrier, limiting ankG's location along the axon. We reasoned that this boundary should have three properties: 1) it should consist of cytoskeletal proteins that occupy regions of the axon mutually exclusive to ankG, 2) it should be assembled before the clustering of ankG, and 3) its development should be ankG-independent.

To identify proteins that satisfy these criteria, we immunostained cultured hippocampal neurons with antibodies against previously reported axonal cytoskeletal proteins including: ankyrinB (ankB), βII spectrin, αII spectrin, microtubule associated protein 1a (MAP1a), neurofilament-H (NF-H), and acetylated tubulin (Boiko et al., 2007; Ogawa et al., 2006; Witte et al., 2008). With the exception of acetylated tubulin, these proteins are located in distal regions of the axon that are mutually exclusive to ankG and βIV spectrin (Figures 2A, 2D, 2G, and S2); line-scans of fluorescence intensity along the axon show ankB and βII spectrin immunofluorescence does not overlap with ankG (Figures 2B and 2E). In addition to the AIS, myelinated axons also exhibit a unique polarized organization with nodal, paranodal, and juxtaparanodal domains characterized by specific ion channels, cell adhesion molecules, and cytoskeletal proteins (Rasband, 2010). Immunostaining of myelinated axons shows that like the AIS, paranodal ankB (Figure 2F), αII spectrin, and βII spectrin (Ogawa et al., 2006) flank nodal ankG. Thus, in axons, the ankB/αII/βII spectrin-based submembranous cytoskeleton occupies regions that are mutually exclusive to ankG.

To determine the temporal expression of ankB and ankG, we performed immunoblotting from cultured hippocampal neurons at 2, 3, 4, and 7 days *in vitro* (DIV). We found that whereas ankB could be detected at every time point examined, ankG protein could be detected only several days after ankB and Neurofilament-M (NFM) (Figure 2C).

We next examined the expression and localization of ankB and βII spectrin during axonogenesis relative to ankG clustering. We immunostained stages 2–5 cultured hippocampal neurons for ankB and ankG. The transition from stage 2 to stage 3 in cultured hippocampal neurons corresponds to the time at which neurons break symmetry, and one neurite becomes longer than another (Kaech and Banker, 2006). Consistent with an early role in cytoskeleton assembly, we found ankB and βII spectrin enriched in a single process (Figure 2H, arrowhead). Similarly, early stage 3 neurons showed a marked enrichment for ankB and βII spectrin at the tip of the growing axon (Figure 2I, arrowhead). However, ankG was not detected at these times of *in vitro* neuronal development (data not shown). Stage 4 neurons had axons strongly labeled with ankB, but not with ankG (Figure 2J, arrowhead). Stage 5 neurons had axons strongly labeled for ankB in the distal axon, and ankG in the proximal axon (Figure 2K, arrowhead). To gain insight into the developmental localization of these different cytoskeletal proteins, we averaged (from 10 different neurons *in vitro*) the ankB, ankG, and βII spectrin fluorescence intensity from 10 μm long line scans at the soma, AIS, axon, and growth cones and consistently found ankB and βII spectrin in the growth cones. Furthermore, we found a strong exclusion of ankB and βII spectrin from the AIS in stage 5 neurons, the time at which ankG is clustered at the AIS (Figures 2M, 2N, and 2O).

Finally, to determine whether axonal targeting of these cytoskeletal proteins depends on ankG, we silenced ankG expression by infection with an adenovirus to express ankG-shRNA, then immunostained for each cytoskeletal protein. We found that in the absence of ankG, neither MAP1a nor NF-H was enriched in the axon (Figures S2B and S2D). In contrast, the axonal targeting of ankB, αII spectrin, βII spectrin, and acetylated tubulin were unaffected (Figures 2L and S2F; αII and βII spectrin not shown). Together, these results indicate that ankB, αII spectrin, and βII spectrin satisfy all the criteria to function as an intra-axonal boundary.

Assembly of an ankyrin/spectrin distal axonal cytoskeleton

Consistent with its role as an obligatory partner for βII spectrin (Bennett and Baines, 2001), we found that αII spectrin, like ankB and βII spectrin, is enriched in the growth cone of developing neurons (Figure 3A). To quantitatively demonstrate the enrichment of ankB, αII spectrin, and βII spectrin in growth cones, we compared the fluorescence intensity of each of these cytoskeletal proteins in the growth cone to their intensity in dendrites (Figure 3B). In contrast, a similar analysis for MAP2 showed that it is not enriched in growth cones.

How do ankB, αII spectrin and βII spectrin become enriched in the axon? To address this question we looked for key protein domains and interactions responsible for their axonal localization. First, we transfected neurons with GFP-tagged chimeras of ankB and ankG (Mohler et al., 2002) where the N-terminal membrane- binding domains (M), the internal spectrin-binding domains (S), and/or the C-terminal regulatory ‘death’ domains (DC) were swapped (Figure 3). Whereas full-length ankB-GFP ($M_BS_BDC_B$) is efficiently targeted to axons (Figures 3C and 3G), ankG-GFP ($M_GS_GDC_G$) is not polarized and is found in both axons and dendrites (Figure 3G; note that we used a 190 kD form of ankG that is not normally targeted to the AIS; Zhang and Bennett, 1998). We found all chimeras that included ankB’s spectrin-binding domain were efficiently targeted to axons (Figures 3D and 3G), but that neither ankB’s membrane- binding domain (M_B), nor its regulatory death domain (DC_B), is sufficient to restrict chimeras to the axon (Figure 3G). Similarly, replacing ankB’s spectrin-binding domain (S_B) with ankG’s spectrin-binding domain (S_G) impaired

the polarized axonal targeting (Figures 3E and 3G). AnkB's interaction with βII spectrin can be disrupted by a single residue substitution (A1000P) in ankB's spectrin-binding domain (Mohler et al., 2004). When we transfected a mutant A1000P-ankB-GFP into neurons, this protein failed to be targeted to axons (Figures 3F and 3G). Our results strongly support the conclusion that ankB's polarization in axons depends on its interaction with βII spectrin.

Since transport of proteins and cargoes necessary for axon growth depends on fast axonal transport by kinesin microtubule motors (e.g. KIF3) (Hirokawa and Takemura, 2005), we searched for motor proteins or motor adaptor proteins that interact with αII spectrin or βII spectrin. Previous studies showed that KIF3 can interact with cargoes through the adaptor protein KAP3 (Yamazaki et al., 1996), and a yeast two-hybrid screen using KAP3 as bait identified αII spectrin as a binding partner (Takeda et al., 2000). Immunostaining stage 3 cultured primary hippocampal neurons showed that KAP3 and KIF3 colocalize with ankB at the tips of growing axons (Figures 3H and 3I, arrowheads). Immunoprecipitation experiments from brain lysates demonstrate the existence of a macromolecular protein complex including αII spectrin, ankB, KIF3, and KAP3 (Figure 3J). In contrast, neither ankG nor βIV spectrin could be co-immunoprecipitated with KIF3 or KAP3 (data not shown). These results suggest that the submembranous cytoskeletal proteins ankB, αII spectrin, and βII spectrin may be transported to the axon by a KAP3/KIF3 microtubule motor protein complex.

Manipulation of the intra-axonal boundary

If ankB, αII spectrin, and βII spectrin form a cytoskeletal boundary or barrier that excludes ankG from the distal axon, then moving the location of the boundary closer to the cell body should result in a shorter ankG-labeled AIS. To test this possibility, we overexpressed ankB-GFP, αII spectrin-GFP, or βII spectrin-GFP in cultured primary hippocampal neurons (Figures 4A–F). We found that overexpression of ankB restricted ankG to a significantly shorter region of the proximal axon (Figures 4A and 4B). However, exogenous αII spectrin-GFP or βII spectrin-GFP were unpolarized (Figures 4C – 4F), and their expression led to significantly longer ankG-labeled AIS (Figures 4B, 4C, and 4E). When we examined ankB in cells overexpressing αII spectrin-GFP or βII spectrin-GFP, we found ankB was even more efficiently localized to the distal axon, leaving a pronounced gap in ankB immunostaining in the proximal axon (Figures 4D and 4F, bracket). We conclude that αII spectrin-GFP and βII spectrin-GFP promote the trafficking of ankB to more distal axonal regions, leading to a distal shift of the boundary and a longer ankG-labeled AIS.

To determine if the temporal sequence of ankB and ankG expression is important for the assembly and/or location of the intra-axonal boundary, we overexpressed GFP-tagged ankG (ankG270-GFP) in hippocampal neurons at DIV 0. We then determined if a boundary between ankG270-GFP and endogenous ankB immunoreactivity formed by DIV 3, and whether the location of this boundary was influenced by the premature expression of exogenous ankG. Importantly, we found that cells with a morphologically identifiable axon had long stretches of axonal ankG270-GFP immunoreactivity that did not overlap with ankB (Figures 4G and 4H). The endogenous ankB was still efficiently trafficked to the axon, but it was restricted to more distal segments. In some instances when ankG was overexpressed, ankB accumulated at the end of the axon in dense aggregates (Figure 4G). By DIV 7, these ankG270-GFP labeled AIS were on average nearly three times the length of the AIS in control neurons (Figures 4B and 4I), and ankB was excluded from these regions with exogenous ankG270-GFP (Figures 4I and 4J). These experiments show that even when over-expressed, ankG and ankB will not occupy the same axonal domains. Furthermore, they suggest that the temporal expression and amounts of ankB, αII spectrin, and βII spectrin are critical determinants of the intra-axonal boundary.

Silencing of ankB, αII spectrin, or βII spectrin in vitro disrupts ankG clustering and AIS assembly

To directly test whether ankB, αII spectrin, and βII spectrin comprise a boundary to restrict ankG to the proximal axon, we silenced expression of these cytoskeletal proteins using adenovirus to introduce shRNAs. We infected neurons at the time of plating, and then waited 7 days for neurons to mature. Infection of neurons resulted in the specific and efficient silencing of each target protein (Figure 4K). To confirm that loss of ankB, αII spectrin, or βII spectrin does not affect axonogenesis and/or neuronal polarity, we examined Tau1 localization and found that it was still enriched in a single process (Figures 4L-4N). However, consistent with their role in axonal targeting of ankB, we found that silencing the expression of αII spectrin or βII spectrin disrupted the localization of ankB (Figures 4O and 4P).

In uninfected cultures nearly all neurons have a well-defined AIS with both ankG and Na+ channels (Figure 5I; Hedstrom et al., 2007). Neurons infected with adenovirus to express GFP alone, or to express GFP and NF-shRNA, also had normal ankG-labeled AIS (Figure 5I). However, in neurons infected with adenovirus to express ankB-shRNA, αII spectrin-shRNA, or βII spectrin-shRNA, ankG clustering at the AIS was disrupted (Figure 5). Instead, we found most neurons lacked ankG clustering (Figures 5A and 5D), and had diffuse ankG located throughout the distal axon (Figures 5B and 5C). We also found neurons where ankG was located in conspicuous puncta, or as a ‘fragmented AIS’ along the axon (Figures 5E–5H). Notably, these puncta contained other AIS proteins including βIV spectrin and NF-186 (Figures 5J and 5K). These puncta were located at the cell surface since extracellular NF-186 antibodies labeled these clusters (Figure 5K). Importantly, as ankB, αII spectrin, and βII spectrin all form a complex, silencing the expression of any single one of these caused a similar disruption of the AIS (Figure 5I), further supporting the conclusion that specific disruption of the distal cytoskeleton is the cause for loss of ankG clustering at the AIS.

As additional evidence that the AIS failed to assemble after silencing of ankB, αII spectrin, or βII spectrin, we examined the distribution of MAP2, since it is efficiently excluded from the axons of cultured neurons by the ankG-based AIS (Hedstrom et al., 2008). Axonal MAP2 was readily detected after silencing of ankB, αII spectrin, or βII spectrin (Figures 5A–5H). These results support the conclusion that the distal axonal cytoskeleton is necessary to restrict ankG to the proximal axon.

AnkG clustering in ankB, αII spectrin, and βII spectrin deficient mice

AnkB-deficient mice (*ANK2 −/−*) die shortly after birth from profound nervous system defects (Scotland et al., 1998). However, when we immunostained *ANK2 +/+* and *ANK2 −/−* brains for ankB, ankG and βIV spectrin, we found normal AIS (Figures 6A and 6B), and we observed no difference in the number average length of AIS (data not shown). These results contrast sharply with our *in vitro* experiments and suggest that 1) additional extrinsic mechanisms exist *in vivo* that contribute to AIS assembly, 2) off-target effects of the ankB shRNAs are responsible for loss of ankG clustering *in vitro*, or 3) that *ANK2 −/−* neurons compensate *in vivo* for loss of ankB through some unknown mechanism. To distinguish among these possibilities, we compared hippocampal neurons cultured from *ANK2 +/+* and *ANK2 −/−* mice and found a significant increase in the length of the ankG-labeled AIS in *ANK2 −/−* neurons (Figure 6C). When we attemped to rescue the defect by transfecting ankB-GFP into *ANK2 −/−* neurons, we found that this reduced AIS length in both *ANK2 +/+* and *ANK2 −/−* neurons (Figure 6C), as was observed previously (Figures 4A and 4B). This result suggests that the increased AIS length observed in cultured *ANK2 −/−* neurons is a specific consequence of loss of ankB, rather than a loss of extrinsic factors.

To determine if the ankB-shRNA used here has off-target effects or if there is compensation by some other unknown protein, we transduced cultured *ANK2 +/+* and *ANK2 −/−* neurons using ankB-shRNA adenovirus. If off-target effects impaired ankG clustering at the AIS, then a similar disruption should be seen in both *ANK2 −/−* and *ANK2 +/+* neurons. However, we found impaired ankG clustering only in *ANK2 +/+* neurons, and not in *ANK2 −/−* neurons (Figures 6D and 6E). These results support the conclusion that *ANK2 −/−* neurons compensate for loss of ankB (N.B., even in control experiments (GFP alone) we observed more mouse neurons with no or fragmented AIS compared to cultured rat neurons).

To determine if *ANK2 −/−* mice require the spectrin-based distal axonal cytoskeleton to restrict ankG to the proximal axon, we silenced αII spectrin and βII spectrin in *ANK2 +/+* and *ANK2 −/−* neurons using adenovirus. We found that as in rat neurons (Figure 5), loss of these two components of the distal axonal cytoskeleton blocked AIS clustering of ankG. We found fragmented ankG or diffusely distributed ankG along the axon (Figures 6F and 6G, arrowheads). When we quantified this effect, we found that silencing of αII and βII spectrin in *ANK2 +/+* neurons caused disruption of AIS ankG clustering in 94.2% and 89.9% of neurons, respectively. Similarly, we found that silencing of αII and βII spectrin in *ANK2 −/−* neurons caused disruption of AIS ankG clustering in 85.2% and 83.9% of neurons, respectively. Thus, although *ANK2 −/−* mice compensate for loss of ankB, a distal submembranous cytoskeleton comprised of αII spectrin and βII spectrin is still required for ankG clustering at the AIS.

To more directly demonstrate the important role of αII spectrin for AIS assembly *in vivo*, we examined brains from αII spectrin-deficient mice (*SPNA2 −/−*). These mice were generated by a β-geo exon trap insertion resulting in an αII spectrin-βgal fusion protein lacking the C-terminus of αII spectrin necessary for heterodimer formation with βII spectrin (Stankewich et al., 2011). *SPNA2 −/−* mice have widespread developmental abnormalities including nervous system and cardiac defects, and embryos die around E15 (Stankewich et al., 2011).

We evaluated brains from embryonic *SPNA2 +/−* and *SPNA2 −/−* mice to determine if ankG is properly clustered at the proximal axon. While cortex from control embryos showed robust αII spectrin immunoreactivity (Figure 6H), *SPNA2 −/−* mice lacked αII spectrin staining (Figure 6I). In control mice, ankG immunostaining showed two prominent layers of AIS (Figure 6H, brackets): one layer near the pial surface with AIS oriented mostly horizontally and likely corresponding to Cajal-Retzius cells, and a second wider layer deeper in the brain with AIS oriented mostly vertically (Figure 6J). Immunostaining of *SPNA2 −/−* cortex also showed two distinct ankG-labeled layers. However, when compared to *SPNA2 +/−* brains, these layers were much broader (Figure 6I, brackets). Specifically, ankG was distributed over wider regions and appeared fragmented in *SPNA2 −/−* mice (Figure 6K). At higher magnification (Figure 6K, boxed regions), ankG was located in discrete puncta and the AIS appeared fragmented (Figure 6L, arrowheads).

Since *SPNA2 −/−* die at E15, and the loss of αII spectrin occurs in all cells in these animals, it is possible the AIS disruption we observed is secondary to the loss of αII spectrin in some other cell type. To demonstrate that disruption of ankG clustering was caused by the absence of αII spectrin specifically in neurons, we electroporated αII spectrin shRNA into embryonic neurons by *in utero* electroporation and monitored their ability to mature and cluster ankG at the AIS. At P28, we found electroporated neurons that arrived in layers II-III of the cortex and that developed both axons and dendrites (Figure 6M). However, when we examined ankG immunoreactivity, we found AIS ankG in αII spectrin-shRNA transfected neurons appeared fragmented (Figure 6N, arrowheads), similar to the pattern observed in

cultured neurons lacking αII spectrin and in *SPNA2 −/−* brains. Whereas 58/58 GFP transfected cells had normal AIS, 22/24 αII spectrin shRNA transfected neurons had fragmented AIS (e.g. Figure 6N), and the remaining 2 neurons had no detectable ankG. Thus, αII spectrin is a component of the distal axonal cytoskeleton that is necessary to properly restrict and cluster ankG at the AIS.

Finally, to demonstrate that disruption of the distal axonal cytoskeleton impairs AIS assembly *in vivo*, we generated mice with a targeted mutation in the *SPNB2* gene for conditional ablation of βII spectrin. We introduced LoxP sites flanking exon 3 of the gene *SPNB2* (*SPNB2*$^{fl/fl}$; Figures 7A and 7B). We crossed these animals with mice expressing Cre under the neuronal promoter Nestin (*Nestin-Cre*) to produce *Nestin-Cre;SPNB2*$^{fl/fl}$ mice (Figure 7B). Both immunoblot analysis (Figure 7C) and immunostaining of cerebellum (Figure 7D) showed that *Nestin-Cre;SPNB2*$^{fl/fl}$ mice lack neuronal βII spectrin. While most *Nestin-Cre;SPNB2*$^{fl/fl}$ mice died by P14, some survived for more than 5 months.

To determine if βII spectrin is important for AIS assembly *in vivo*, we immunostained brains from *SPNB2*$^{fl/fl}$ and *Nestin-Cre;SPNB2*$^{fl/fl}$ mice using antibodies against βIV spectrin and ankG. We found that as in *SPNA2 −/−* mice, AIS in *Nestin-Cre;SPNB2*$^{fl/fl}$ mice were significantly disrupted compared to control *SPNB2*$^{fl/fl}$ mice (Figures 7E–F). In CA1 region of the hippocampus, high densities of AIS are found in a discrete layer as the output of pyramidal neurons. While *SPNB2*$^{fl/fl}$ mice had a normal layer of AIS (Figure 7E, between dotted lines), it was severely disrupted in *Nestin-Cre;SPNB2*$^{fl/fl}$ mice (Figure 7F). Furthermore, there were many puncta of βIV spectrin and ankG immunoreactivity in the distal axons of these pyramidal neurons (Figure 7F, below dotted lines). When AIS were still observed in *Nestin-Cre;SPNB2*$^{fl/fl}$ mice they had fragmented βIV spectrin and ankG immunoreactivities that extended beyond the distal end of the AIS (Figure 7G, arrowheads). These observations were not limited to the hippocampus as we also found significant fragmentation and disruption of AIS in the cortex (data not shown). These results demonstrate that the distal axonal cytoskeletal proteins αII spectrin and βII spectrin are essential for the proper restriction and clustering of ankG to the AIS.

DISCUSSION

AnkG is required to maintain neuronal polarity and to recruit every known AIS protein, including the ion channels responsible for action potential initiation (Rasband, 2010). However, the mechanisms responsible for ankG clustering at the AIS, and ankG's role in establishing polarity remain unknown. Here, we have addressed two main questions: 1) what is the relationship between ankG clustering and neuronal polarity, and 2) how does ankG get restricted to the AIS? We found that ankG is dispensable for axon specification, and that ankG's localization at the AIS depends on an intra-axonal boundary defined by the distal axonal cytoskeleton.

AnkG and the establishment of neuronal polarity

Using *in utero* electroporation we showed that ankG clustering follows axon specification. In contrast to its importance in maintenance of polarity, ankG is not required to establish polarity. The difference in ankG's functions in immature and mature neurons may be related to the observation that maintenance of polarity depends on an intact actin cytoskeleton (Winckler et al., 1999). Lipids and membrane proteins have much reduced mobility in the AIS membrane of mature neurons, and this reduced mobility depends on actin (Nakada et al., 2003). The AIS diffusion barrier is not functional until after ankG is located at the AIS, suggesting that AIS accumulation of actin occurs after ankG clustering (Brachet et al., 2010). Actin likely accumulates at the AIS through its interaction with βIV spectrin, which is recruited to the AIS through binding to ankG (Yang et al., 2007). Together our results are

consistent with the idea that during early development a polarity and axon specification program actively determines which neurite becomes the axon (Barnes and Polleux, 2009), and this program functions independently of ankG. However, in mature neurons with a fully specified axon and AIS, we speculate that this polarity program is downregulated and nonfunctional, and polarity is instead maintained by the ankG-dependent AIS cytoskeleton (Hedstrom et al., 2008).

An intra-axonal boundary limiting ankG to the AIS

An AIS barrier restricts the diffusion of membrane proteins and lipids, and inhibits the axonal trafficking of dendritic cytoplasmic cargoes (Rasband, 2010). Nevertheless, how the AIS functions as a barrier remains poorly understood. The data presented here reveal the existence of a second, more distal barrier, or boundary, which functions at the level of the submembranous cytoskeleton to restrict ankG to the AIS. This boundary consists of a membrane-associated lattice-like meshwork of ankB, αII spectrin, and βII spectrin (Bennett and Baines, 2001).

How is the distal cytoskeleton assembled? We showed that at the time of axon specification, ankB, αII spectrin, and βII spectrin are enriched at the growth cone (Figure 7H, *i*), and then fill the distal region of the developing axon (Figure 7H, *ii*). AnkB's axonal localization requires interaction with βII spectrin, and our data suggest that the ankB/αII spectrin/βII spectrin complex becomes enriched in the axon by transport along microtubules through interactions with microtubule motors and their adaptors like KIF3 and KAP3. Disruption of KIF3 function blocks axonogenesis (Nishimura et al., 2004), and stabilization of microtubules promotes the development of multiple axons (Witte et al., 2008). Future experiments will determine whether other motor and adaptor proteins also contribute to assembly of the distal axonal cytoskeleton.

We propose that the ankB/αII spectrin/βII spectrin distal cytoskeleton forms by 'backfilling' of the axon, in a distal to proximal manner, due to strong trafficking mechanisms that direct these proteins to the axon. The distal submembranous cytoskeleton is assembled and can be detected before ankG clustering at the AIS. Upon expression of ankG, we speculate that it, too, is strongly targeted to the axon, perhaps through a similar set of interactions with motor proteins and adaptors. Like the distal cytoskeleton, the ankG-based AIS is assembled in a distal to proximal manner (Figures 1 and 7, *ii–iv*).

Why is ankG not detected in the distal axon? Our data do not demonstrate that ankG does not enter into the distal axon, but rather that ankG cannot integrate into the distal submembranous cytoskeleton, resulting in apparent exclusion from the distal axon. This may reflect differences in affinity between ankG and βII spectrin compared to ankB and βII spectrin (Komada and Soriano, 2002), structural differences between ankG-spectrin complexes and ankB-spectrin complexes, differences in trafficking efficiency, or a combination of these. AnkG's inability to integrate into the distal cytoskeleton results in the generation of an apparent intra-axonal boundary, or barrier, established by the ankB/αII spectrin/βII spectrin-based submembranous cytoskeleton (Figure 7H, *v*). Thus, the only site where ankG and βIV spectrin can begin to form a submembranous cytoskeletal network is in the most proximal axon where ankB/αII spectrin/βII spectrin are not found. This model suggests that the temporal regulation and amounts of ankG and ankB are at least partially responsible for the location of the apparent boundary. The results from experiments where we overexpressed ankB or ankG are consistent with this interpretation, since overexpression of ankB results in a proximal shift of the boundary, while early ankG expression results in a dramatic distal shift of the boundary (Figure 7H, *vi–vii*). Furthermore, upon silencing of any component of the distal cytoskeleton, the boundary is disrupted and ankG and its binding

partners can be located in distal regions of the axon far from where the AIS is normally found (Figure 7H, *viii*).

An intra-axonal barrier or boundary has previously been shown to exist in *Drosophila*, where it restricts the location of axon guidance molecules to distinct distal and proximal domains (Katsuki et al., 2009). We speculate that the intra-axonal barrier observed in *Drosophila* axons and the ankB/αII spectrin/βII spectrin intra-axonal barrier we describe here derive from a common precursor. However, the molecular nature of the barrier in *Drosophila* is unknown. It will be interesting to determine if *Drosophila* ankyrin or spectrin mutants have disrupted localization of distal and/or proximal guidance molecules.

Although our *in vitro* data demonstrate that loss of any component of the distal cytoskeleton including ankB, αII spectrin, or βII spectrin disrupts ankG clustering, experiments in *ANK2 −/−* neurons suggest that there is a hierarchy for these distal cytoskeletal proteins and their requirement for the establishment of an intra-axonal barrier. This conclusion is based on the observation that other, as yet unidentified, proteins can substitute for ankB, but not for αII spectrin and βII spectrin, since both *SPNA2 −/−* and *Nestin-Cre;SPNB2$^{fl/fl}$* mice have disrupted ankG clustering. Recently, two human mutations in αII spectrin were identified that cause early-onset West syndrome with cerebral hypomyelination (Saitsu et al., 2010). Although these mutations result in proteins that still assemble as heterodimers with βII spectrin, when expressed in heterologous cells they formed intracellular aggregates of both αII and βII spectrin. Our experiments provide an explanation for why the mutant αII spectrins disrupt nervous system function.

AnkG clustering at nodes of Ranvier

If the distal ankB/αII spectrin/βII spectrin-based submembranous cytoskeleton blocks the assembly of an ankG/βIV spectrin-based cytoskeleton in the distal axon, how can ankG become clustered at nodes of Ranvier that are evenly spaced along the axon? We propose that clustering of the ankG-binding cell adhesion molecule NF-186 (Davis et al., 1996) by myelinating glial cells at developing nodes permits the nucleation of an ankG/βIV-spectrin based submembranous cytoskeleton in the distal axon. Since ankG is found at nodes far from the AIS, the intra-axonal boundary cannot be a strict barrier that excludes trafficking of ankG to the distal axon, but instead supports the idea that ankG cannot be incorporated into the submembranous cytoskeleton unless there is some attachment site such as NF-186. Indeed, neurofascin-deficient mice cannot cluster ankG at nascent nodes, but they still cluster ankG at the AIS (Sherman et al., 2005). The paranodal cytoskeleton may also contribute to ankG clustering and/or stability by assembling submembranous cytoskeletal barriers that restrict the location of ankG and its binding partners between every paranodal junction (Feinberg et al., 2010; Ogawa et al., 2006). Thus, in myelinated nerve fibers the ankB/αII spectrin/βII spectrin submembranous cytoskeleton may be viewed as repeating intra-axonal boundaries restricting the location of ankG to key sites necessary for action potential generation and propagation.

Axon initial segment plasticity

Neuronal activity can modulate the position and length of the AIS, and this can impact neuronal excitability (Grubb and Burrone, 2010; Kuba et al., 2010). However, the mechanisms underlying AIS plasticity remain unknown. Our results show the ankB/αII spectrin/βII spectrin-based distal cytoskeleton can determine the location of ankG, and suggest the intra-axonal barrier may contribute to the plasticity of AIS length and position. Future experiments will determine if remodeling of the distal cytoskeleton by activity-dependent mechanisms is responsible for altered AIS structure and function.

In conclusion, our results suggest a novel mechanism that contributes to development of the polarized organization of the axonal membrane: a mechanism that relies on exclusion of cytoskeletal proteins rather than active clustering.

EXPERIMENTAL PROCEDURES

Antibodies

A detailed list of antibodies and their sources can be found in the Supplemental Experimental Procedures.

Plasmids

pEGFP 220-kDa ankB and 190-kDa ankG chimeric expression constructs were previously described (Mohler et al., 2002). The A1000P point mutant was generated by site-directed mutagenesis. The ankB-GFP and ankG270-GFP were a kind gift from Dr. Vann Bennett (Duke University). For overexpression experiments, we also used αII-spectrin-GFP, and βII-spectrin-GFP. For *in utero* electroporation, pCx-EGFP (CAG promoter driving EGFP expression) was used to study the formation of the AIS in developing neurons. The ankG-shRNA used for electroporation was previously described (Hedstrom et al., 2007).

Hippocampal culture and Transfection

A detailed description of the procedures for culture and transfection is found in the Supplemental Experimental Procedures.

In Utero Electroporation

For in vivo experiments, *in utero* electroporation was performed as previously described (Hedstrom et al., 2007). Plasmids were introduced into rat or mouse embryos at E16 or E14, respectively. After recovery of the mother, embryos and new born pups were sacrificed at the indicated times for immunostaining.

Generation of βII spectrin conditional knockout mice

The *SPNB2* gene has multiple alternatively spliced mRNAs. The conditional knockout strategy was designed to excise exon 3 upon Cre-mediated excision. Details of the targeting construct and screening strategies can be found in the Supplemental Experimental Procedures. *SPNB2*$^{fl/+}$ mice were crossed with *Nestin-Cre* mice to excise the floxed exon, resulting in βII spectrin-deficient mice.

Immunofluorescence and image analysis

Cultured neurons were immunostained and imaged as described previously (Ogawa et al., 2010). Additional details can be found in the Supplemental Experimental Procedures.

Immunoprecipitation

Immunoprecipitation experiments were performed from whole mouse brains as previously described (Ogawa et al., 2010). For immunoblots made from neuronal cultures, cells were briefly rinsed and scraped from coverslips in PBS containing protease inhibitors. Cells were then centrifuged at 12000 rpm for 10 min at 4°C and lysed 1% Triton-X lysis buffer (Ogawa et al., 2010). Protein concentration was determined and samples were boiled (95°C, 5 min) or heated (37°C, 15 min) in reducing sample buffer, separated by SDS-PAGE and analysed by immunoblot.

Statistics

All statistical analyses were performed using GraphPad Prism software or Microsoft Excel.

Supplementary Material

Refer to Web version on PubMed Central for supplementary material.

Acknowledgments

We thank Dr. Ed Cooper and the Rasband lab for discussions and critical reading of the manuscript. This research was supported by NIH grants NS044916 (MNR), NS069688 (MNR), HL083422 (PJM), and HL084583 (PJM), the Dr. Miriam and Sheldon Adelson Medical Research Foundation, and Mission Connect. The generation of the *SPNB2*$^{fl/fl}$ micewas supported in part by Baylor College of Medicine IDDRC Grant Number 5P30HD024064-23 from the Eunice Kennedy Shriver National Institute Of Child Health & Human Development. The content is solely the responsibility of the authors and does not necessarily represent the official views of the Eunice Kennedy Shriver National Institute Of Child Health & Human Development or the National Institutes of Health.

References

Barnes AP, Polleux F. Establishment of axon-dendrite polarity in developing neurons. Annu Rev Neurosci. 2009; 32:347–381. [PubMed: 19400726]

Bennett V, Baines AJ. Spectrin and ankyrin-based pathways: metazoan inventions for integrating cells into tissues. Physiol Rev. 2001; 81:1353–1392. [PubMed: 11427698]

Boiko T, Vakulenko M, Ewers H, Yap CC, Norden C, Winckler B. Ankyrin-dependent and -independent mechanisms orchestrate axonal compartmentalization of L1 family members neurofascin and L1/neuron-glia cell adhesion molecule. J Neurosci. 2007; 27:590–603. [PubMed: 17234591]

Brachet A, Leterrier C, Irondelle M, Fache MP, Racine V, Sibarita JB, Choquet D, Dargent B. Ankyrin G restricts ion channel diffusion at the axonal initial segment before the establishment of the diffusion barrier. J Cell Biol. 2010; 191:383–395. [PubMed: 20956383]

Davis JQ, Lambert S, Bennett V. Molecular composition of the node of Ranvier: identification of ankyrin-binding cell adhesion molecules neurofascin (mucin+/third FNIII domain−) and NrCAM at nodal axon segments. Journal of Cell Biology. 1996; 135:1355–1367. [PubMed: 8947556]

Dzhashiashvili Y, Zhang Y, Galinska J, Lam I, Grumet M, Salzer JL. Nodes of Ranvier and axon initial segments are ankyrin G-dependent domains that assemble by distinct mechanisms. J Cell Biol. 2007; 177:857–870. [PubMed: 17548513]

Feinberg K, Eshed-Eisenbach Y, Frechter S, Amor V, Salomon D, Sabanay H, Dupree JL, Grumet M, Brophy PJ, Shrager P, Peles E. A glial signal consisting of gliomedin and NrCAM clusters axonal Na+ channels during the formation of nodes of Ranvier. Neuron. 2010; 65:490–502. [PubMed: 20188654]

Garrido JJ, Giraud P, Carlier E, Fernandes F, Moussif A, Fache MP, Debanne D, Dargent B. A targeting motif involved in sodium channel clustering at the axonal initial segment. Science. 2003; 300:2091–2094. [PubMed: 12829783]

Grubb MS, Burrone J. Activity-dependent relocation of the axon initial segment fine-tunes neuronal excitability. Nature. 2010

Hedstrom KL, Ogawa Y, Rasband MN. AnkyrinG is required for maintenance of the axon initial segment and neuronal polarity. J Cell Biol. 2008; 183:635–640. [PubMed: 19001126]

Hedstrom KL, Xu X, Ogawa Y, Frischknecht R, Seidenbecher CI, Shrager P, Rasband MN. Neurofascin assembles a specialized extracellular matrix at the axon initial segment. J Cell Biol. 2007; 178:875–886. [PubMed: 17709431]

Hill AS, Nishino A, Nakajo K, Zhang G, Fineman JR, Selzer ME, Okamura Y, Cooper EC. Ion channel clustering at the axon initial segment and node of ranvier evolved sequentially in early chordates. PLoS Genet. 2008; 4:e1000317. [PubMed: 19112491]

Hirokawa N, Takemura R. Molecular motors and mechanisms of directional transport in neurons. Nat Rev Neurosci. 2005; 6:201–214. [PubMed: 15711600]

Kaech S, Banker G. Culturing hippocampal neurons. Nat Protoc. 2006; 1:2406–2415. [PubMed: 17406484]

Kaphzan H, Buffington SA, Jung JI, Rasband MN, Klann E. Alterations in intrinsic membrane properties and the axon initial segment in a mouse model of angelman syndrome. J Neurosci. 2011; 31:17637–17648. [PubMed: 22131424]

Katsuki T, Ailani D, Hiramoto M, Hiromi Y. Intra-axonal patterning: intrinsic compartmentalization of the axonal membrane in Drosophila neurons. Neuron. 2009; 64:188–199. [PubMed: 19874787]

Kole MH, Stuart GJ. Signal processing in the axon initial segment. Neuron. 2012; 73:235–247. [PubMed: 22284179]

Komada M, Soriano P. [Beta]IV-spectrin regulates sodium channel clustering through ankyrin-G at axon initial segments and nodes of Ranvier. J Cell Biol. 2002; 156:337–348. [PubMed: 11807096]

Kuba H, Oichi Y, Ohmori H. Presynaptic activity regulates Na(+) channel distribution at the axon initial segment. Nature. 2010

Mohler PJ, Gramolini AO, Bennett V. The ankyrin-B C-terminal domain determines activity of ankyrin-B/G chimeras in rescue of abnormal inositol 1,4,5-trisphosphate and ryanodine receptor distribution in ankyrin-B (−/−) neonatal cardiomyocytes. J Biol Chem. 2002; 277:10599–10607. [PubMed: 11781319]

Mohler PJ, Yoon W, Bennett V. Ankyrin-B targets beta2-spectrin to an intracellular compartment in neonatal cardiomyocytes. J Biol Chem. 2004; 279:40185–40193. [PubMed: 15262991]

Nakada C, Ritchie K, Oba Y, Nakamura M, Hotta Y, Iino R, Kasai RS, Yamaguchi K, Fujiwara T, Kusumi A. Accumulation of anchored proteins forms membrane diffusion barriers during neuronal polarization. Nat Cell Biol. 2003; 5:626–632. [PubMed: 12819789]

Nishimura T, Kato K, Yamaguchi T, Fukata Y, Ohno S, Kaibuchi K. Role of the PAR-3-KIF3 complex in the establishment of neuronal polarity. Nat Cell Biol. 2004; 6:328–334. [PubMed: 15048131]

Ogawa Y, Oses-Prieto J, Kim MY, Horresh I, Peles E, Burlingame AL, Trimmer JS, Meijer D, Rasband MN. ADAM22, a Kv1 channel-interacting protein, recruits membrane-associated guanylate kinases to juxtaparanodes of myelinated axons. Journal of Neuroscience. 2010; 30:1038–1048. [PubMed: 20089912]

Ogawa Y, Schafer DP, Horresh I, Bar V, Hales K, Yang Y, Susuki K, Peles E, Stankewich MC, Rasband MN. Spectrins and ankyrinB constitute a specialized paranodal cytoskeleton. J Neurosci. 2006; 26:5230–5239. [PubMed: 16687515]

Pan Z, Kao T, Horvath Z, Lemos J, Sul JY, Cranstoun SD, Bennett MV, Scherer SS, Cooper EC. A common ankyrin-G-based mechanism retains KCNQ and Nav channels at electrically active domains of the axon. Journal of neuroscience. 2006; 26:2599–2613. [PubMed: 16525039]

Rasband MN. The axon initial segment and the maintenance of neuronal polarity. Nat Rev Neurosci. 2010

Saitsu H, Tohyama J, Kumada T, Egawa K, Hamada K, Okada I, Mizuguchi T, Osaka H, Miyata R, Furukawa T, et al. Dominant-negative mutations in alpha-II spectrin cause West syndrome with severe cerebral hypomyelination, spastic quadriplegia, and developmental delay. Am J Hum Genet. 2010; 86:881–891. [PubMed: 20493457]

Schafer DP, Jha S, Liu F, Akella T, McCullough LD, Rasband MN. Disruption of the axon initial segment cytoskeleton is a new mechanism for neuronal injury. J Neurosci. 2009; 29:13242–13254. [PubMed: 19846712]

Scotland P, Zhou D, Benveniste H, Bennett V. Nervous system defects of AnkyrinB (−/−) mice suggest functional overlap between the cell adhesion molecule L1 and 440-kD AnkyrinB in premyelinated axons. J Cell Biol. 1998; 143:1305–1315. [PubMed: 9832558]

Sherman DL, Tait S, Melrose S, Johnson R, Zonta B, Court FA, Macklin WB, Meek S, Smith AJ, Cottrell DF, Brophy PJ. Neurofascins are required to establish axonal domains for saltatory conduction. Neuron. 2005; 48:737–742. [PubMed: 16337912]

Sobotzik JM, Sie JM, Politi C, Del Turco D, Bennett V, Deller T, Schultz C. AnkyrinG is required to maintain axo-dendritic polarity in vivo. Proc Natl Acad Sci U S A. 2009; 106:17564–17569. [PubMed: 19805144]

Song AH, Wang D, Chen G, Li Y, Luo J, Duan S, Poo MM. A selective filter for cytoplasmic transport at the axon initial segment. Cell. 2009; 136:1148–1160. [PubMed: 19268344]

Stankewich MC, Cianci CD, Stabach PR, Ji L, Nath A, Morrow JS. Deletion of alphaII spectrin disrupts cell organization, growth, and neural and cardiac development. Journal of Cell Science. 2011

Takeda S, Yamazaki H, Seog DH, Kanai Y, Terada S, Hirokawa N. Kinesin superfamily protein 3 (KIF3) motor transports fodrin-associating vesicles important for neurite building. J Cell Biol. 2000; 148:1255–1265. [PubMed: 10725338]

Winckler B, Forscher P, Mellman I. A diffusion barrier maintains distribution of membrane proteins in polarized neurons. Nature. 1999; 397:698–701. [PubMed: 10067893]

Witte H, Neukirchen D, Bradke F. Microtubule stabilization specifies initial neuronal polarization. J Cell Biol. 2008; 180:619–632. [PubMed: 18268107]

Yamazaki H, Nakata T, Okada Y, Hirokawa N. Cloning and characterization of KAP3: a novel kinesin superfamily-associated protein of KIF3A/3B. Proc Natl Acad Sci U S A. 1996; 93:8443–8448. [PubMed: 8710890]

Yang Y, Ogawa Y, Hedstrom KL, Rasband MN. {beta}IV spectrin is recruited to axon initial segments and nodes of Ranvier by ankyrinG. J Cell Biol. 2007; 176:509–519. [PubMed: 17283186]

Zhang X, Bennett V. Restriction of 480/270-kD ankyrin G to axon proximal segments requires multiple ankyrin G-specific domains. J Cell Biol. 1998; 142:1571–1581. [PubMed: 9744885]

Zhou D, Lambert S, Malen PL, Carpenter S, Boland LM, Bennett V. AnkyrinG is required for clustering of voltage-gated Na channels at axon initial segments and for normal action potential firing. J Cell Biol. 1998; 143:1295–1304. [PubMed: 9832557]

Zonta B, Desmazieres A, Rinaldi A, Tait S, Sherman DL, Nolan MF, Brophy PJ. A Critical Role for Neurofascin in Regulating Action Potential Initiation through Maintenance of the Axon Initial Segment. Neuron. 2011; 69:945–956. [PubMed: 21382554]

RESEARCH HIGHLIGHTS

- AnkyrinG clustering follows and is dispensable for axon specification
- A distal cytoskeleton defines an intra-axonal boundary limiting ankG to the AIS
- Disruption of the distal cytoskeleton blocks ankyrinG clustering and AIS assembly
- αII and βII spectrin deficient mice have disrupted AIS

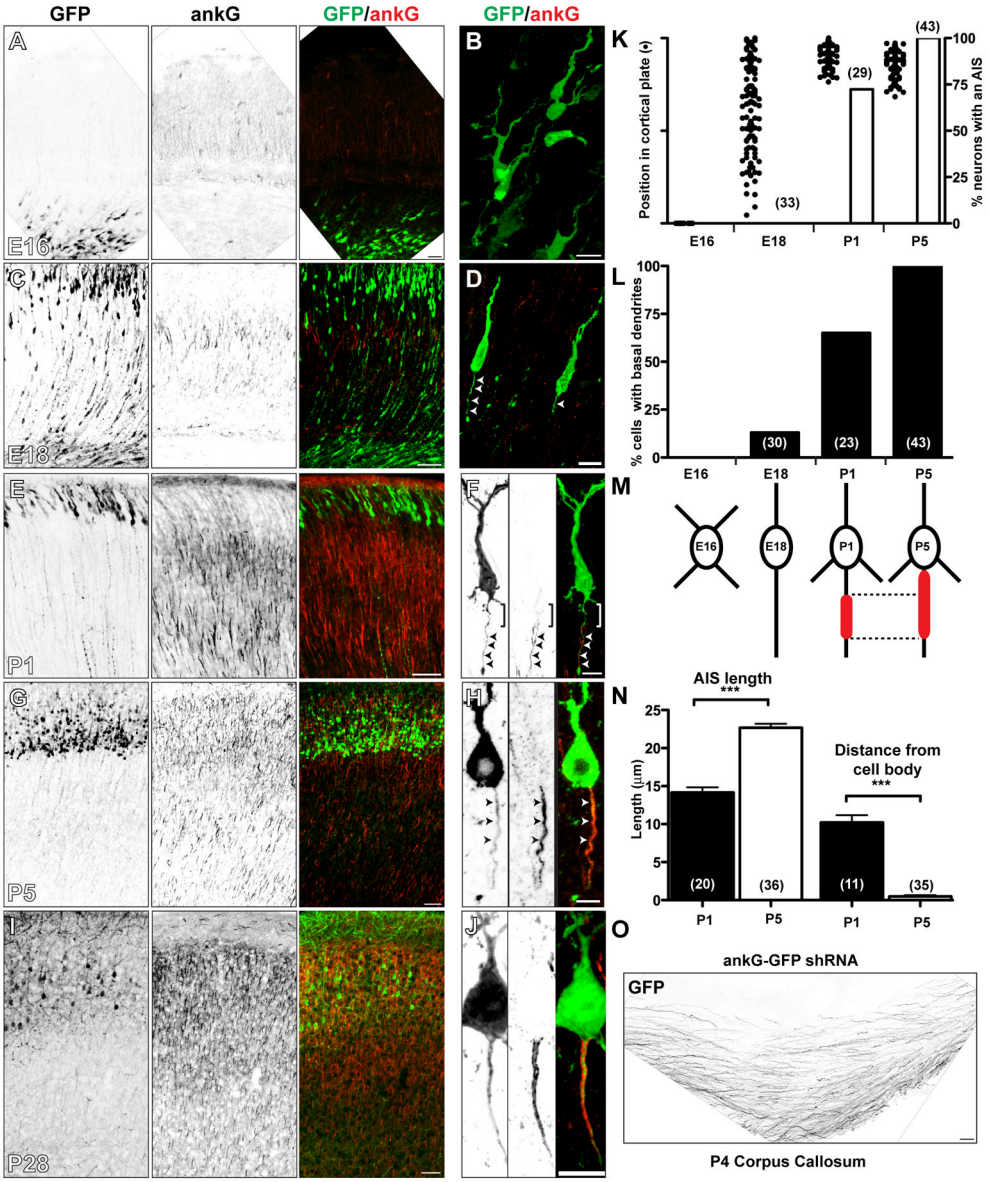

Figure 1. AnkG clustering follows and is dispensible for axon specification

(A–J) Neurons electroporated in utero at E14 with GFP plasmids and immunostained for GFP (green) and ankG (red) at embryonic day 16 (E16) (A, B), E18 (C, D), postnatal day 1 (P1) (E, F), P5 (G, H), and P28 (I, J). Scale bars: A, 25 μm; B, D, F, J, 10 μm; C, E, G, I, 50 μm; H, 5 μm.

(K) The percentage of GFP-electroporated neurons with an AIS defined by ankG (vertical bars) and their positions in the cortical plate (dots). The number of cells analyzed is indicated in parentheses.

(L) The percentage of GFP-electroporated neurons with basal dendrites.

(M) Cartoon illustrating the transition in cellular morphology, the position and length of ankG along the axon.

(N) The length and distance from the cell body of the ankG-labeled AIS.

(O) GFP-labeled axons from neurons expressing the ankG-shRNA construct cross the *corpus callosum*. Scale bar, 50 μm.

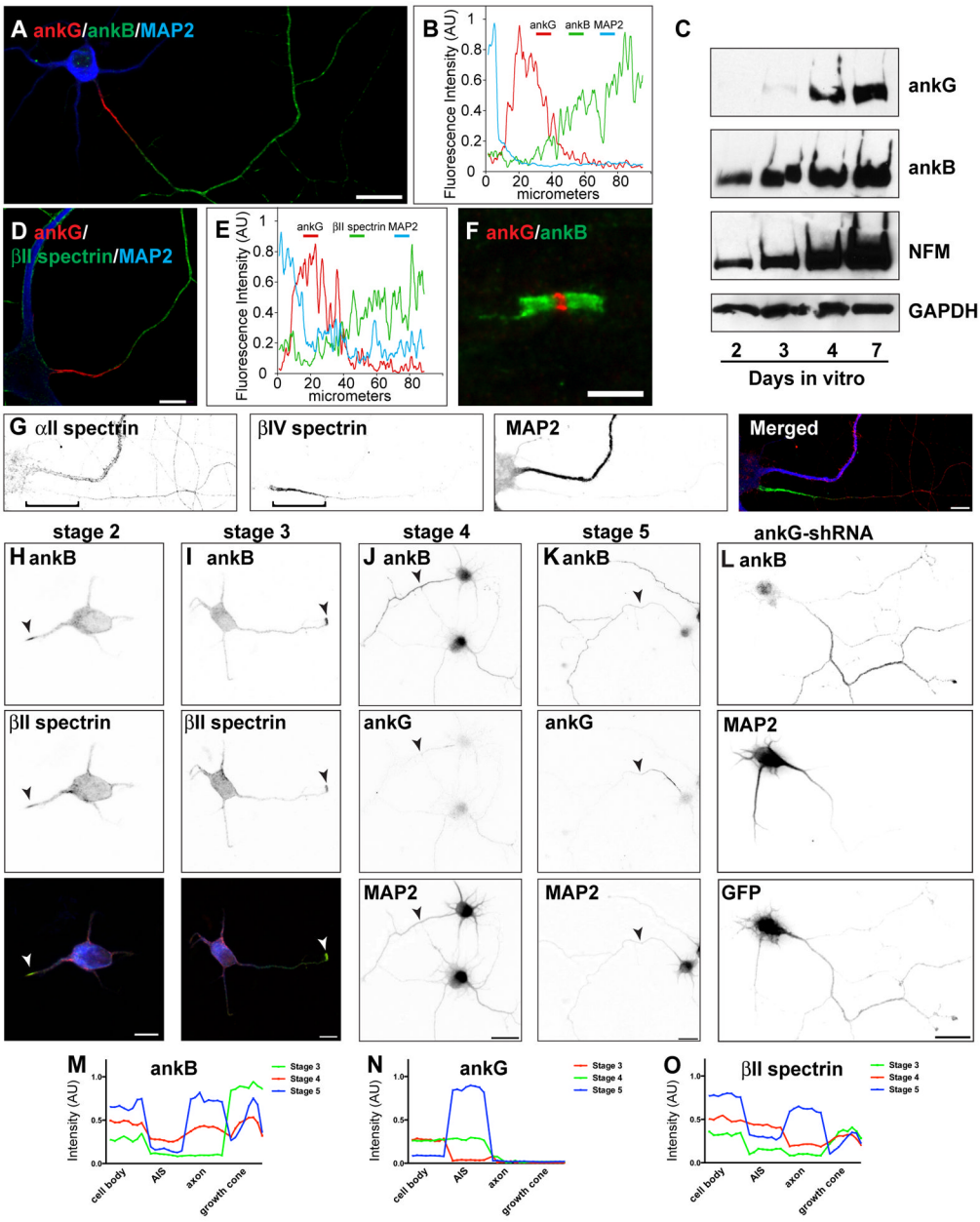

Figure 2. AnkB, αII spectrin, and βII spectrin comprise a distal submembranous cytoskeleton assembled before ankG clustering

(A) Immunostaining of a 10 DIV hippocampal neuron for MAP2 (blue), ankG (red), and ankB (green). Scale bar, 20 μm.

(B) Line-scan of fluorescence intensity along the axon shown in (A).

(C) Immunoblot analysis of cultured hippocampal neurons. Immunoblotting was performed for ankG, ankB, Neurofilament M (NFM), and GAPDH as a loading control.

(D) Immunostaining of a 10 DIV hippocampal neuron labeled for MAP2 (blue), ankG (red), and βII spectrin (green). Scale bar, 10 μm.

(E) Line-scan of fluorescence intensity along the axon shown in (D).

(F) Node of Ranvier immunostained for ankG (red) and ankB (green). Scale bar, 5 μm.

(G) Immunostaining of a 10 DIV hippocampal neuron labeled for αII spectrin (red), βIV spectrin (green), and MAP2 (blue). Scale bar, 10 μm.
(H–I) AnkB (green) and βII spectrin (red) are enriched at the tips of newly specified axons (arrowheads). In the merged image, MAP2 is shown in blue. Scale bar, 10 μm.
(J–K) Immunostaining for ankB, ankG, and MAP2. Arrowheads indicate axons. Scale bar, 20 μm.
(L) Cultured hippocampal infected with ankG-shRNA adenovirus at DIV 0, and analyzed at 7 DIV. AnkB is enriched in axons lacking ankG. Scale bar, 20 μm.
(M–O) Fluorescence intensity measurements for ankB, ankG, and βII spectrin taken from the soma, AIS, axon, and growth cone.

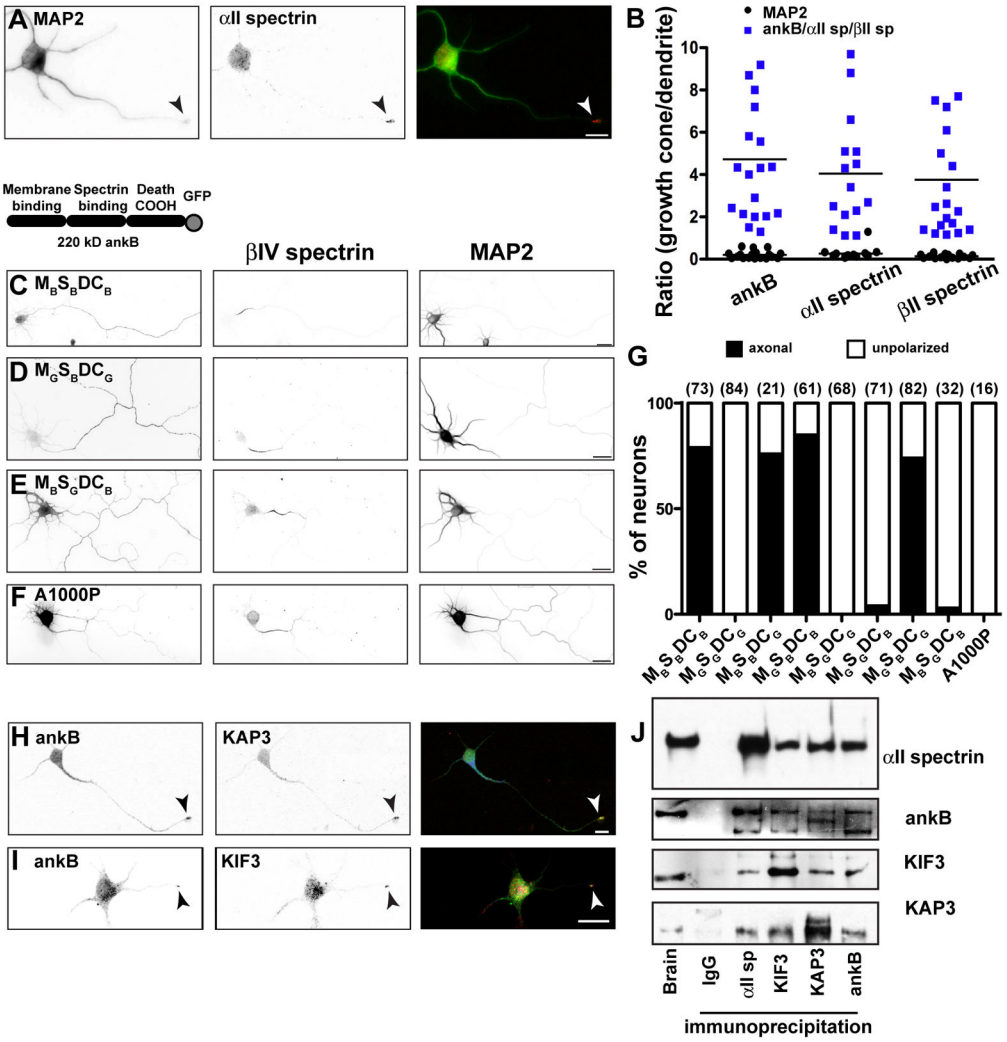

Figure 3. Developmental assembly of the distal axonal cytoskeleton

(A) Stage 3 hippocampal neuron labeled for MAP2 (green) and αII spectrin (red). The arrowhead indicates the growth cone. Scale bar, 10 μm.

(B) The ratio of growth cone to dendrite fluorescence intensity for ankB, αII spectrin, and βII spectrin immunofluorescence (blue squares).

(C–E) Cultured hippocampal neurons transfected with 220 kD ankB-GFP ($M_BS_BDC_B$), or chimeras of ankB-GFP and ankG-GFP, and labeled for GFP, βIV spectrin and MAP2. The analysis was performed at 7 DIV. Scale bar, 25 μm.

(F) Cultured hippocampal neuron transfected with A1000P ankB-GFP, and labeled for GFP, βIV spectrin, and MAP2. The analysis was performed at 7 DIV. Scale bar, 25 μm.

(G) Quantification of axonal polarity using ankB and ankG chimeras. The number of cells analyzed is shown in parentheses.

(H, I) Stage 3 hippocampal neuron labeled for ankB (green) and KAP3 (H; red) or KIF3 (I; red). The arrowhead indicates the growth cone. Scale bar, 10 μm.

(J) Immunoprecipitation reactions from brain lysates using antibodies against αII spectrin, ankB, KIF3, and KAP3.

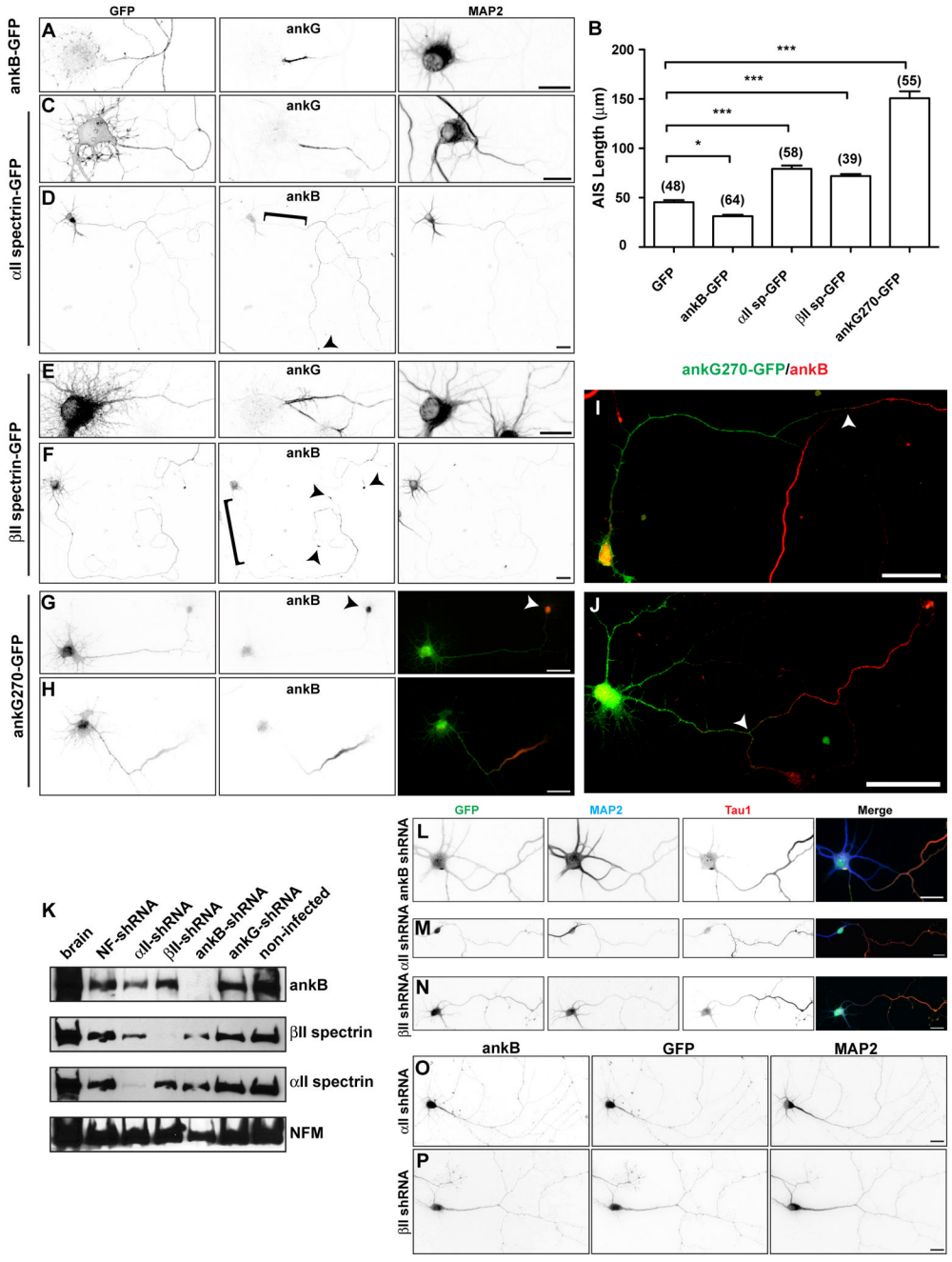

Figure 4. Overexpression of ankyrins and spectrins shifts the intra-axonal barrier

(A) Cultured hippocampal neuron transfected with ankB-GFP at DIV 0 and immunostained for GFP, ankG, and MAP2 at DIV 7. Scale bar, 20 μm.

(B) Quantification of AIS length (ankG immunoreactivity) after transfection of the indicated proteins.

(C–D) Cultured hippocampal neuron transfected with αII spectrin-GFP at DIV 0 and immunostained for GFP, ankG (C) or ankB (D), and MAP2 at DIV 7. Brackets indicate the proximal axon, and arrowheads indicate the growth cone. Scale bar, 20 μm.

(C) (E–F) Cultured hippocampal neuron transfected with βII spectrin-GFP at DIV 0 and immunostained for GFP, ankG (C) or ankB (D), and MAP2 at DIV 7. Brackets indicate the proximal axon, and arrowheads indicate the growth cone. Scale bar, 20 μm.
(G–H) Cultured hippocampal neurons transfected with ankG270-GFP at DIV 0, immunolabeled for GFP and ankB at DIV 3. Arrowhead in (G) indicates the end of the axon. Scale bar, 25 μm.
(I-J) Cultured hippocampal neurons transfected with ankG270-GFP at DIV 0, immunolabeled for GFP and ankB (at DIV 7). Arrowheads indicate the location of the intra-axonal boundary. Scale bar, 50 μm.
(K) Immunoblots of DIV 7 cultured hippocampal neurons infected with adenovirus to silence expression of the indicated proteins. Each lane corresponds to proteins from two replicate wells. Neurofilament-M (NFM) was used as a loading control.
(L–N) Hippocampal neurons infected at DIV 0 with adenovirus to silence expression of ankB (L), αII spectrin (M), and βII spectrin (N), and labeled for GFP (green), MAP2 (blue), and Tau1 (red) at DIV 7. Scale bars, 25 μm.
(O–P) Hippocampal neurons infected at DIV 0 with adenovirus to silence expression of αII spectrin (O) or βII spectrin (P), and labeled for ankB, GFP, and MAP2 at DIV 7. Scale bars, 25 μm.

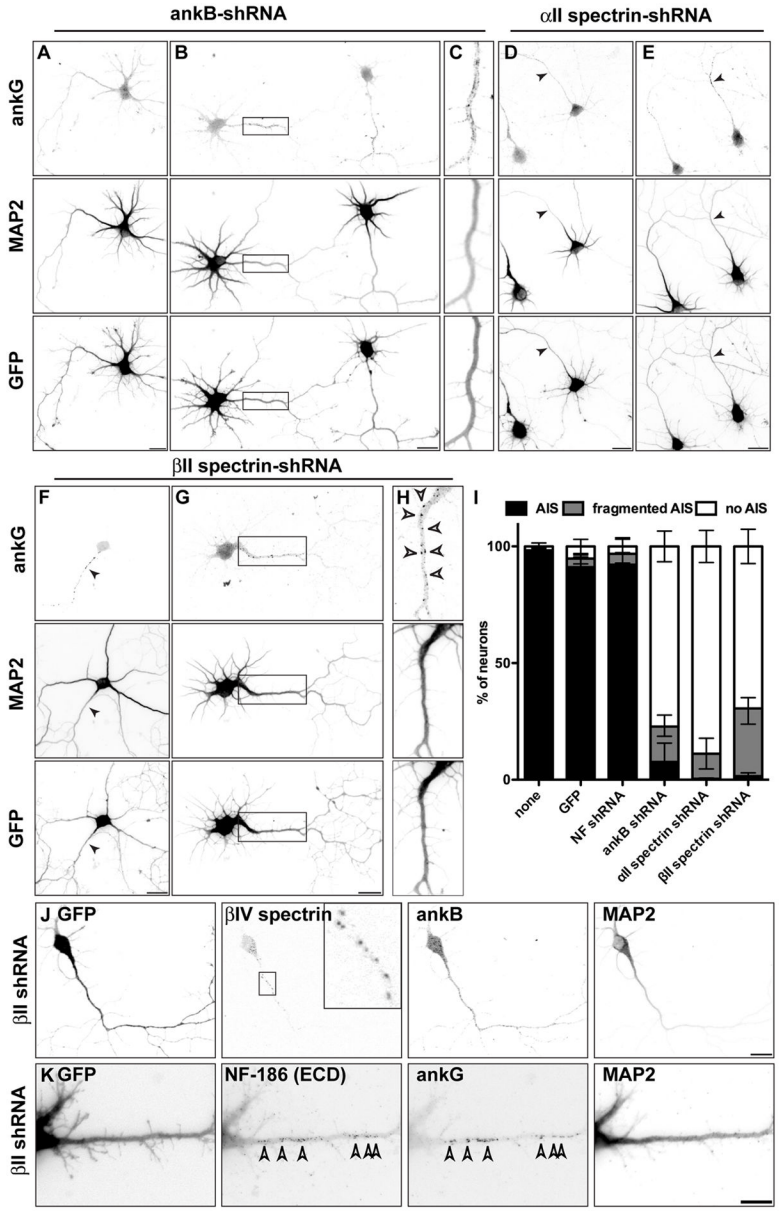

Figure 5. Loss of ankB, αII spectrin, or βII spectrin inhibits ankG clustering

(A–H) Hippocampal neurons infected at DIV 0 with ankB-shRNA (A–C), αII spectrin-shRNA (D–E), and βII spectrin-shRNA (F–H) adenovirus and immunostained for ankG, MAP2, and GFP at DIV7. Boxes in (B) and (G) corresponds to panels (C) and (H), respectively. Scale bars, 20 μm.

(I) Quantification of the staining patterns for ankG. Data are mean ± SD. The total number of neurons counted was 467 (none), 402 (GFP), 426 (NF shRNA), 571 (ankB shRNA), 502 (αII spectrin shRNA), and 526 (βII spectrin shRNA).

(J–K) Neurons infected at DIV 0 with βII spectrin-shRNA adenovirus and immunostained for GFP, βIV spectrin, ankB, and MAP2 (J) or GFP, NF-186 ectodomain (ECD), ankG, and MAP2 (K) at DIV 7. Scale bars, 20 μm.

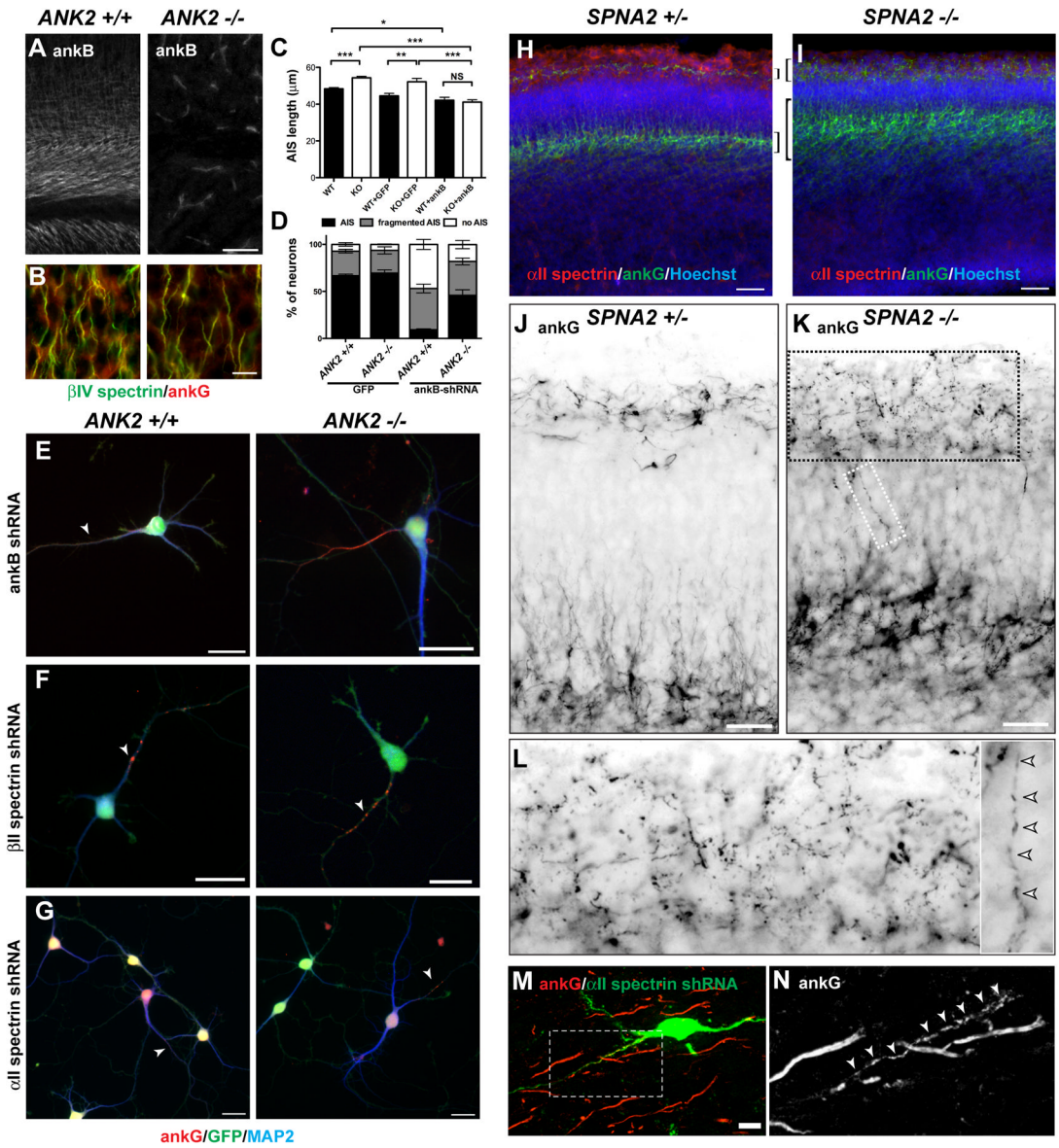

Figure 6. Analysis of ankB-deficient (*ANK2* −/−) and αII spectrin-deficient (*SPNA2* −/−) mice

(A) AnkB immunostaining of *ANK2 +/+* and *ANK2 −/−* mice. Scale bar, 25 μm.

(B) βIV spectrin (green) and ankG (red) immunostaining of *ANK2 +/+* and *ANK2 −/−* cortex. Scale bar, 10 μm.

(C) AIS length at 7 DIV from *ANK2 +/+* and *ANK2 −/−* neurons *in vitro* untransfected, or transfected with GFP or ankB-GFP. Error bars indicate ±SEM. *** P < 0.0001; ** P < 0.001; * P < 0.01; NS, not significant.

(D) The percentage of *ANK2 +/+* and *ANK2 −/−* neurons with a normal, fragmented, or no AIS after viral transduction to express GFP or ankB shRNA. Error bars indicate ±SEM.

(E–G) Immunostaining of hippocampal neurons from *ANK2 +/+* and *ANK2 −/−* mice after silencing of ankB (E), βII spectrin (F), or αII spectrin (G). All neurons shown were transduced and GFP+. Arrows indicate fragmented AIS. Scale bars, 20 μm.

(H–I) E15 cortex from *SPNA2 +/−* (H) and *SPNA2 −/−* (I) mice immunostained for αII spectrin (red), ankG (green), and Hoechst (blue). Brackets indicate cortical layers with high levels of ankG immunoreactivity. Scale bars, 50 μm.

(J–K) E15 cortex from *SPNA2 +/−* (J) and *SPNA2 −/−* (K) mice immunostained for ankG (green). The regions shown span the two main layers labeled by ankG as shown in panels (H–I).. Scale bars, 25 μm.

(L) Higher magnification images from boxed regions in panel (K) show fragmented ankG immunoreactivity (arrowheads).

(M) αII spectrin shRNA-electroporated neurons at P28 labeled for GFP (green) and ankG (red). Scale bar, 10 μm.

(N) Boxed region from (M) showing fragmented ankG immunoreactivity.

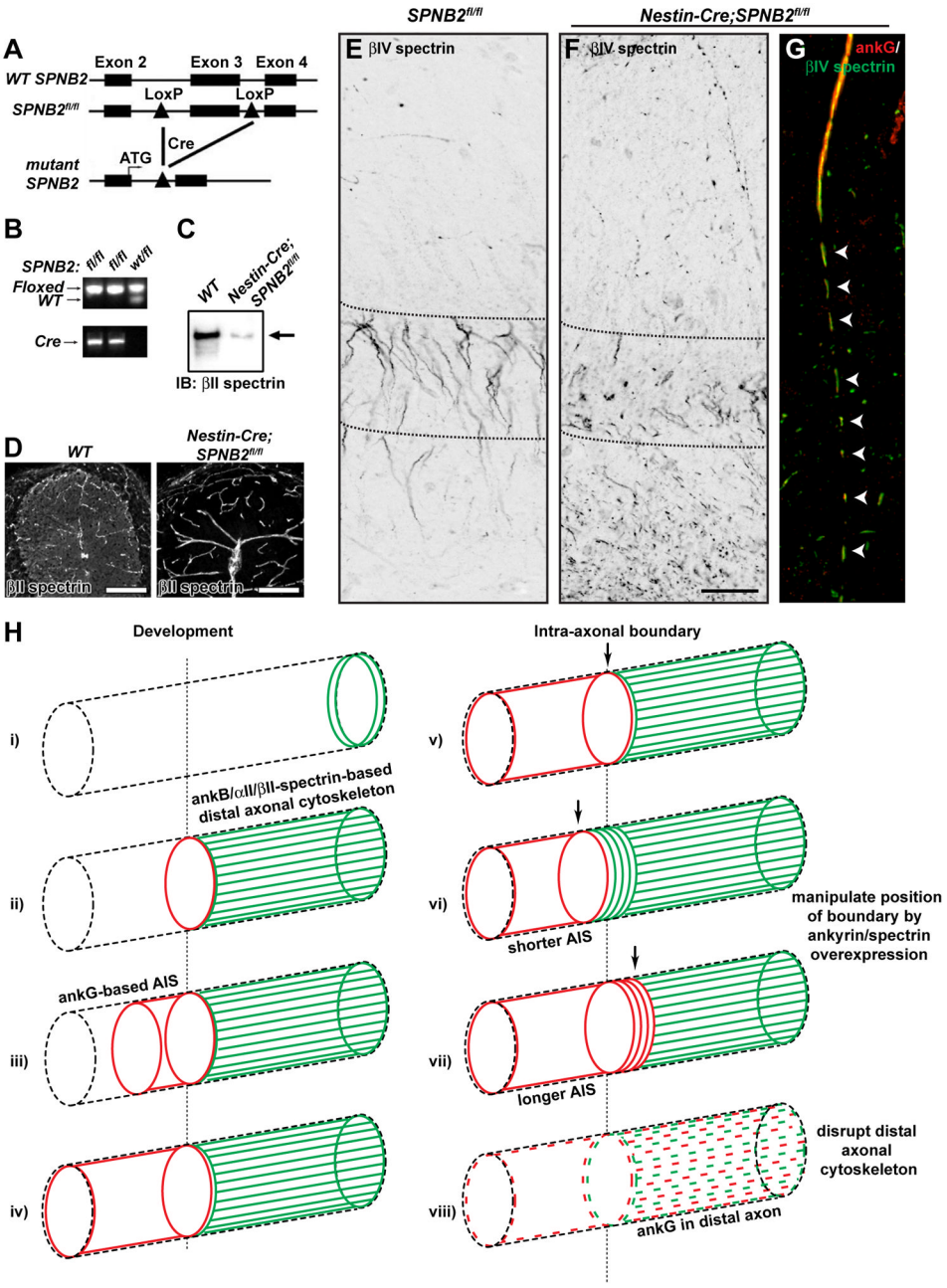

Figure 7. Analysis of a nervous system specific βII spectrin-deficient mouse

(A) Schematic representation of the genomic wild-type *SPNB2 (WT SPNB2*), floxed (*SPNB2*$^{fl/fl}$), and mutant loci.

(B) PCR analysis of genomic tail DNA of mutant (*fl/fl*) or heterozygous (*wt/fl*) mice.

(C) Immunoblot analysis of βII spectrin in brain lysates from wild-type (*WT*) or *Nestin-Cre;SPNB2*$^{fl/fl}$ mice.

(D) βII spectrin immunostaining of *WT* and *Nestin-Cre;SPNB2*$^{fl/fl}$ cerebellum. High levels of βII spectrin immunoreactivity remain in the vasculature. Scale bar, 100 μm.

(E–F) βIV spectrin labeling of *SPNB2*$^{fl/fl}$ (E) and *Nestin-Cre;SPNB2*$^{fl/fl}$ hippocampus. Scalebar, 50 μm.

(G) AnkG (red) and βIV spectrin (green) Immunostaining of *Nestin-Cre;SPNB2*$^{fl/fl}$ axon. Arrowheads indicate the fragmented AIS.

(H) *i)* AnkB, αII spectrin, and βII spectrin are located in the distal growth cone during axonogenesis. *ii*) AnkB, αII spectrin, and βII spectrin comprise a distal axonal cytoskeleton that is assembled before ankG clustering. *iii*) AnkG accumulates at the distal end of the future AIS, at the boundary with the distal axonal submembranous cytoskeleton. *iv*) AnkG fills and defines the AIS in a distal to proximal direction. *v*) The transition from ankG/βIV spectrin to ankB/αII spectrin/βII spectrin along the axon defines the intra-axonal boundary. *vi*) Overexpression of ankB causes a proximal shift of the intra-axonal boundary and a shorter AIS. *vii*) Overexpression of ankG causes a distal shift of the intra-axonal boundary and a longer AIS. *viii*) Loss of the intra-axonal boundary by disruption of the distal axonal cytoskeleton blocks AIS assembly and permits ankG to be found in the distal axon.